KRAS phosphorylation regulates cell polarization and tumorigenic properties in colorectal cancer

Débora Cabot[1,2], Sònia Brun[1,2], Noelia Paco[1,2], Mireia M. Ginesta[3], Núria Gendrau-Sanclemente[1,8], Baraa Abuasaker[1,2] Triana Ruiz-Fariña[1], Carles Barceló[1,2,9], Miriam Cuatrecasas[2,4,], Marta Bosch[1,2], Carles Rentero[1,2], Gabriel Pons[6], Josep M Estanyol[1,7], Gabriel Capellà[3], Montserrat Jaumot[1,2]*, Neus Agell[1,2]*.

[1] Dept. Biomedicina, Facultat de Medicina i Ciències de la Salut, Universitat de Barcelona., Barcelona, Spain.

[2] Institut d'Investigacions Biomèdiques August Pi i Sunyer (IDIBAPS), Barcelona, Spain.

[3] Hereditary Cancer Program, Translational Research Laboratory, Catalan Institute of Oncology, ICO-IDIBELL, Hospitalet de Llobregat, Barcelona, Spain and Centro de Investigación Biomédica en Red en Cáncer (CIBERONC), Madrid, Spain.

[4] Departament de Fonaments Clínics, Facultat de Medicina i Ciències de la Salut, Universitat de Barcelona; Pathology Department and Centro de Investigación Biomédica en Red de Enfermedades Hepáticas y Digestivas (CIBERehd) and Tumor Bank-Biobank, Hospital Clínic, Barcelona, Spain.

[6]Departament de Ciències Fisiològiques, Facultat de Medicina i Ciències de la Salut, Universitat de Barcelona and Institut d'Investigació Biomèdica de Bellvitge (IDIBELL), L'Hospitalet de Llobregat, Barcelona, Spain.

[7]Proteomics Unit, CCiT-UB, University of Barcelona, Barcelona, Spain.

[8]Present address: Program Against Cancer Therapeutic Resistance (ProCURE), Catalan Institute of Oncology, Hospital Duran i Reynals, Institut d'Investigació Biomèdica de Bellvitge (IDIBELL), L'Hospitalet de Llobregat, Barcelona, Spain.

[9]Present address: Institut d'Investigació Sanitària Illes Balears (IdISBa), Palma de Mallorca, Spain.

Keywords

RAS / *CTNNA1* / *HNF4G* / *SERPINE1* / *PRSS2* / *NEO1*

*Corresponding authors:

Neus Agell Jané: neusagell@ub.ub; Montserrat Jaumot Pijoan: mjaumot@ub.edu

Abstract

Oncogenic mutations of KRAS are found in the most aggressive human tumors, including colorectal cancer. It has been suggested that oncogenic KRAS phosphorylation at Ser181 modulates its activity and favors cell transformation. Using non-phosphorylatable (S181A), phosphomimetic (S181D) and phospho/dephosphorylatable (S181) oncogenic KRAS mutants, we analyzed the role of this phosphorylation to the maintenance of tumorigenic properties of colorectal cancer cells. Our data show that the presence of phospho/dephosphorylatable oncogenic KRAS is required for preserving the epithelial organization of colorectal cancer cells in 3D cultures, and for supporting subcutaneous tumor growth in mice. Interestingly, gene expression differed according to the phosphorylation status of KRAS. In DLD-1 cells, CTNNA1 was only expressed in phospho/dephosphorylatable oncogenic KRAS expressing cells, correlating with cell polarization. Moreover, lack of oncogenic KRAS phosphorylation leaded to changes in expression of genes related to cell invasion, such as *SERPINE1, PRSS1,2,3* and *NEO1,* and expression of phosphomimetic oncogenic KRAS resulted in diminished expression of genes involved in enterocyte differentiation, such as *HNF4G.* Finally, the analysis, in a public data set of human colorectal cancer, of the gene expression signatures associated to phosphomimetic and non-phosphorylatable oncogenic KRAS suggests that this post-translational modification regulates tumor progression in patients.

Introduction

KRAS is a member of the Ras family of small GTPases. Its wild type form cycles from the inactive (GDP-bound) to the active (GTP-bound) state, responding faithfully to extracellular signals. When GTP-bound, it interacts with effector proteins that activate diverse signal transduction pathways, which in turn regulate processes such as proliferation, survival or differentiation in normal cells, the best studied being the c-RAF/MEK/ERK and PI3K/AKT[1]. All RAS isoforms have a highly conserved globular domain that contains the catalytic lobe and the allosteric lobe; and the non-conserved C-terminal domain, the hypervariable region (HVR), which contains the membrane targeting signals[2]. RAS proteins are irreversibly modified by farnesylation in the cysteine of the C-terminal CAAX sequence. Uniquely, adjacent to this modified aminoacid, KRAS has also a stretch of six contiguous lysines , which promotes an electrostatic interaction with the negatively-charged phosphate groups of phospholipids[3].

RAS is a major oncogenic driver in a variety of tumor types. Oncogenic KRAS mutations are found in the most deadly cancers (pancreatic (91%), colorectal (CRC, 42%), and lung (33%))[1,4]. Although oncogenic mutations preserve KRAS in its GTP-bound state, diverse evidences suggest that oncogenic KRAS can be regulated, and so there may be several factors that maintain GTP-bound KRAS in a non-signaling state[5–7].

Non-effector proteins that bind to the HVR or/and the allosteric lobe of KRAS, such as PDE6-δ[5], galectin 3[8], calmodulin (CaM)[9–11], HNRNPA2B1[12], nucleophosmin[13] and β-catenin[14], are examples of proteins that can modulate oncogenic KRAS activity s[6,8,15,16]. Additionally, several post-translational modifications of KRAS such as phosphorylation, ubiquitination or acetylation have been reported to be also able to modulate oncogenic KRAS activity[6,16–21]; among them, phosphorylation at Ser181, within the HVR, is the most studied. We demonstrated that this phosphorylation is regulated by CaM interaction[6] and that expression of phosphomimetic mutants of oncogenic KRAS in normal mouse fibroblasts favored activation of downstream signaling, cell transformation, and tumor growth in mouse models[6,12,18]. Our data obtained in DLD-1 cells deleted for the endogenous oncogenic KRAS allele and overexpressing exogenous non-phosphorylatable or phosphorylatable oncogenic KRAS at Ser181 also confirmed the role

of S181 phosphorylation for CRC tumor growth[18]. It has also been described using other cellular models, that KRAS phosphorylation induces apoptosis[20] and that non-phosphorylated KRAS, by capturing CaM, inhibits the non-canonical Wnt/Ca2+ signaling and promotes tumorigenicity[19]. These contrasting results may be due to the use of different cellular models but may also be due to the distinct expression levels of the oncogenic KRAS.

Although it is widely accepted that KRAS is a good target for cancer therapy, its inhibition represents a challenge. Interfering with its post-translational modifications such as phosphorylation at Ser181 may open a new therapeutic opportunity, but first, the relevance of this phosphorylation in the maintenance of the tumorigenic properties of established cancer cells must be demonstrated. To this end, we have generated CRC cells expressing different oncogenic KRAS phosphomutants. Our data show that the presence of phospho/dephosphorylatable oncogenic KRAS is essential for maintaining the polarity of the CRC cells and for allowing tumor growth, and interestingly, that the presence of non-phosphorylatable oncogenic KRAS impairs the invasive capacity of cells. Thus, we conclude that CRC cells depend on KRAS phosphorylation at Ser181 to maintain their tumorigenic properties.

Results

Colorectal cancer cells expressing different oncogenic KRAS phosphomutants show different epithelial morphology in 2D culture

To study the role of oncogenic KRAS phosphorylation at Ser181 in CRC, DLD-1 cells were used. These cells carry an oncogenic mutant KRAS allele and a wild type (WT) KRAS allele. This cell line was chosen because it depends on the expression of the oncogenic allele of KRAS to fulfill its tumorigenic properties; thus, the isogenic DLD-1 cell line knocked out for the oncogenic KRAS allele (named DLD-1 KO in this paper) does not grow properly under growth factor limiting conditions and does not generate tumors when subcutaneously injected in mice[22,23]. DLD-1 KO cells were transfected to generate clones of cells with recovered expression of oncogenic KRAS, but with different mutations at position 181. Consequently, clones of cells expressing different levels of exogenous oncogenic non-phosphorylatable KRAS (KRAS-S181**A**), oncogenic phosphomimetic KRAS (KRAS-S181**D**) or the control oncogenic phospho/dephosphorylatable KRAS (KRAS-**S**181) were obtained. When examined by phase-contrast microscopy, and regardless of the phosphomutant, all cells with high levels of expression of oncogenic KRAS showed a mesenchymal morphology, while clones expressing oncogenic KRAS at levels like endogenous KRAS maintained an epithelial-like morphology (Fig. 1a and Supplementary Fig. S1a).

To analyze the role of oncogenic KRAS phosphorylation in CRC cells, we chose clones that expressed oncogenic KRAS phosphomutants at levels comparable to those of the endogenous WT KRAS (Fig. 1a, upper panel). Interestingly, although in 2D cultures all clones showed an epithelial-like morphology, clear differences between them were observed. Similar to the original DLD-1 (Supplementary Fig. S1b), cells expressing oncogenic KRAS-**S**181 were able to form compact clusters, in which the boundaries between the cells were barely perceptible (Fig. 1a, bottom panel). Conversely, this type of cell organization was not observed with the oncogenic KRAS-S181**A** and KRAS-S181**D** clones. Furthermore, oncogenic KRAS-S181**D**

cells were rounder than the rest. In conclusion, the phosphorylation status of oncogenic KRAS is relevant for establishing a specific cell morphology in this CRC cell line.

Oncogenic KRAS expression induces cell proliferation and modulates ERK and AKT activation regardless of the Ser181 phosphorylation status of KRAS

To study the relevance of KRAS phosphorylation in cell viability under serum-limiting conditions, cell growth at 0.1 % Fetal Bovine Serum (FBS) was determined for DLD-1, DLD-1 KO and the different oncogenic KRAS phosphomutants (Fig. 1b). As expected, DLD-1 KO cells grew less than DLD-1[22,23] and cells expressing oncogenic KRAS-**S**181 recovered the ability to grow under serum-limiting conditions. Both oncogenic KRAS-S181**A** and KRAS-S181**D** clones grew significantly more than DLD-1 KO cells and similarly to oncogenic KRAS-**S**181 and DLD-1, indicating that growth under starvation was independent of the phosphorylation status of KRAS. In agreement with the proliferation data, the levels of P-AKT and P-ERK in the different oncogenic KRAS phosphomutants were similar to those in DLD-1 cells (Fig. 1c). Therefore, the effect of the constitutively expression of oncogenic KRAS in these CRC cells on the activation of ERK1, 2 and AKT was independent of its phosphorylation status at Ser181. In addition, these data confirmed that the oncogenic KRAS phosphorylation mutants were functional proteins. Similar results in growth and signaling were obtained in all oncogenic KRAS-expressing cells cultured at serum-saturating conditions (Supplementary Fig. S1c,d).

Phosphorylation status of oncogenic KRAS differentially regulates gene expression in colorectal cancer cells

To better understand the phenotypes observed in DLD-1 cells expressing the different oncogenic KRAS phosphomutants, we analyzed and compared their gene expression. Clustering analysis of the differentially expressed genes demonstrated distinct expression patterns between the phosphomutant clones. The greatest differences were found between oncogenic KRAS-S181**A** and KRAS-S181**D** clones (Fig. 2a, b, Supplementary Table S1 and Supplementary Fig.

S2a). Although few, the existence of differentially expressed genes between oncogenic KRAS-S181**A** and KRAS-**S**181 clones indicates that a proportion of KRAS is phosphorylated, and plays a role in the regulation of gene expression (Fig. 2b, cand Supplementary Table S1). Levels of oncogenic KRAS-**S**181 phosphorylation were indirectly estimated by measuring its affinity to CaM[9,19]. Two out of the three oncogenic KRAS-**S**181 clones tested presented a reduced binding to CaM, indirectly corroborating oncogenic KRAS phosphorylation in those **S**181 clones (Supplementary Fig. S2b).

Genes related to enterocyte differentiation such as *HNF4G*, *HEPH*, *MUC13*, and *UGT1A* [24–27] were particularly downregulated in oncogenic KRAS-S181**D** cells compared to both oncogenic KRAS-**S**181 and KRAS-S181**A** (Fig. 2c and Supplementary Fig. S2a), suggesting that KRAS phosphorylation induces a de-differentiation program. Changes in *HNF4G* expression were corroborated by qPCR and Western Blot (WB) (Fig. 2d and Supplementary Fig. S2c, d). Furthermore, GSEA indicated that the expression signature of oncogenic KRAS-S181**D** versus oncogenic KRAS-S181**A** and –**S**181 expressing cells is similar to that of DLD-1 cells with upregulated *LEF1* (Fig. 2e), a gene related to the WNT signaling pathway and pluripotency[28]. *TRIB2*, recently proposed as an oncogene in CRC[29], showed increased expression in cells with the phosphomimetic mutant, as demonstrated by qPCR (Fig. 2d and Supplementary Fig. S2d).

Genes differentially expressed in oncogenic KRAS-S181**A** vs KRAS–**S**181 clones are involved in cell invasion and vascular co-option[30,31]. Specifically, *PRSS1,2,3* (coding for different isoforms of trypsin), and *SERPINE1* (coding for PAI-I) are among the genes whose expression was specifically inhibited more than 2-fold when oncogenic KRAS could not be phosphorylated (Fig. 2c). Furthermore, *NEO1* (codifying for neogenin 1), a suppressor of wound-healing response [32], is the only gene whose expression was significantly increased more than 2-fold in oncogenic KRAS-S181**A**-expressing cells (Fig. 2c). Decreased mRNA levels of *SERPINE1* and *PRSS2* were corroborated by qPCR (Fig. 2d and Supplementary Fig. S2d), and increased levels of neogenin 1 were corroborated by WB (Supplementary Fig. S2c).

CTNNA1 was the only gene whose expression decreased in either S181**A** or S181**D** oncogenic KRAS-expressing cells compared with KRAS-**S**181 (Fig. 2c). This result was confirmed by

qPCR and WB (Fig. 2d, Supplementary Fig. S2d and Fig. 3a). Interestingly, the product of *CTNNA1*, α-E-catenin, is involved in cell-to-cell adhesion, a characteristic that we found to be impaired in cells expressing either the S181**A** or the S181**D** mutants of oncogenic KRAS (Fig. 1a, bottom panel).

Phosphorylation status of KRAS affects both organization of cells growing in 3D cultures and cell invasion capacity

Since α-E-catenin is involved in cell-to-cell adhesion and polarization, we aimed to analyze a possible impact of oncogenic KRAS phosphorylation status in cell growth and organization in 3-Dimensional (3D) culture.

When grown in soft agar, although there was variability between clones, all oncogenic KRAS phosphomutants had a significantly higher capacity to form colonies than DLD-1 KO cells (Supplementary Fig. S3a). Interestingly, the morphology of cell colonies expressing phospho/dephosphorylatable oncogenic KRAS differed from those expressing either oncogenic KRAS-S181**A** or KRAS-S181**D**. While colonies of cells expressing the **S**181 oncogene were compact spheres, colonies of non-phosphorylatable or phosphomimetic mutant cells were non-compact and flatter, with well-distinguished limits between cells (Supplementary Fig. S3b). Growth in Matrigel-based 3D cultures was then analyzed. DLD-1 KO cells formed smaller cellular aggregates than the cell lines expressing oncogenic KRAS (Fig. 3b and Supplementary Fig. S3c). Interestingly, while the three oncogenic KRAS-**S**181 clones formed large, compact spheroidal and organized structures with a central hollow, all oncogenic KRAS-S181**A** or KRAS-S181**D** clones assembled into disorganized and branched "grape-like" aggregates (Fig. 3b). Cells expressing the phosphomimetic oncogenic KRAS were the ones less aggregated.

Immunofluorescence analysis showed that cells expressing oncogenic KRAS-**S**181 formed an epithelial structure of polarized cells with a central lumen. E-cadherin positive contacts between cells could be observed, and polymerized actin was localized in the apical cortex (near the lumen) resembling a structure containing microvilli (Fig. 3c). Finally, α6-integrin was confined

to the basal part of the cells (Fig. 3c). In contrast, all these markers indicated that cells expressing phosphomimetic or non-phosphorylatable oncogenic KRAS were not polarized. These data suggest that the lack of a phosphorylation-dephosphorylation cycle of oncogenic KRAS interfered with the polarization of the cells and, consequently, with the formation of an organized epithelial structure. Finally, immunofluorescence analysis of Matrigel cultures demonstrated that, in cells expressing the phospho/dephosphorylatable KRAS mutant, α-E-catenin was localized at the plasma membrane and mainly in the areas of contact between the cells while it was undetectable in the phosphomimetic and non-phosphorylatble mutant cells. (Fig. 3c).

The fact that, as mentioned above (Fig. 2b, c and Supplementary Table S1), the few differentially expressed genes in oncogenic KRAS-S181**A** vs KRAS-**S**181 clones were related to cell invasion, prompted us to study the impact of the lack of KRAS phosphorylation on cell invasiveness capacity. To test it, we used SW480 cells harboring oncogenic mutations in the two KRAS alleles and being a CRC cell line more prone to invade than DLD-1 cells. Interestingly, the single mutation S181**A** in one of the KRAS alleles leaded to a diminished expression of *SERPINE1* as demonstrated by qPCR (Fig. 4a) and WB (Fig. 4b), and to a reduced invasive capacity (Fig. 4c). Lack of α-E-catenin and increased neogenin-1 expression were also corroborated by either qPCR or WB in these cells (Fig. 4a, b).

Tumor growth is impaired in cells expressing oncogenic non-phosphorylatable or phosphomimetic KRAS

To test whether the phosphorylation status of oncogenic KRAS was also relevant to support tumor growth in CRC cells, DLD-1 KO cells and oncogenic KRAS phosphomutants were subcutaneously injected into nude mice, and tumor growth was monitored over time (Fig. 5a, b and Supplementary Fig. S4a). As expected, DLD-1 KO cells generated very few tumors, which were almost imperceptible macroscopically. In accordance with the previous data obtained with immortalized mouse fibroblasts[18], CRC cells expressing oncogenic KRAS-**S**181 developed subcutaneous tumors, while tumor growth was clearly impaired in oncogenic KRAS-S181**A**

cells. But surprisingly, tumor growth was also reduced in CRC cells expressing oncogenic KRAS-S181**D** (Fig. 5b and Supplementary Fig. S4a).

Interestingly, the histological comparation of the tumors revealed differences in cell organization similar to those observed in cells growing in 3D cultures. While oncogenic KRAS-**S**181-expressing cells formed well-organized epithelial structures around blood vessels, the oncogenic KRAS-S181**A** and KRAS-S181**D** tumors were less differentiated, composed by cells that were poorly organized around smaller or collapsed blood vessels (Fig. 5c and Supplementary Fig. S4b). This lack of organization around the blood vessels could be one of the causes of impaired growth of tumors derived from KRAS-S181**D** and S181**A**-expressing epithelial CRC cells. In fact, WB analysis showed that CA-IX expression was higher in tumors derived from these cells, indicating higher levels of hypoxia (Supplementary Fig. S4c). Furthermore, IHC analysis showed a different distribution of CA-IX signal in the area around the blood vessels (Supplementary Fig. S4b). In the oncogenic KRAS-**S1**81 ones we observed a clear hypoxic negative area around the blood vessels, followed by a strong positive region containing CA-IX positive hypoxic cells, while in the oncogenic KRAS-S181**A** and -S181**D**-derived tumors, hypoxic cells were found much near to the blood vessels.

Lack of α-E-catenin in tumors expressing phosphomimetic or non-phosphorylatable oncogenic KRAS was confirmed (Fig. 5d). A reduction in the amount of trypsin protein was also observed in non-phosphorylatable mutant-derived tumors (Fig. 5d).

Histological analysis showed that tumors generated by all KRAS phosphomutants, presented areas composed of apoptotic and necrotic cells which were TUNEL positive, as well as regions of high cell proliferation which were Ki-67 positive (Supplementary Fig. S4b). The mitotic count in the proliferating areas of all tumors was similar (Supplementary Fig. S4b, d). Finally, the effect of oncogenic KRAS phosphorylation on c-RAF/MEK/ERK and PI3K/AKT signaling pathways in the tumors was similar to that observed in 2D cultures (Fig. 5e). Furthermore, no correlation was observed between tumor growth and the activation status of these two signal transduction pathways.

To generalize the need of KRAS phosphorylation and dephosphorylation for cell polarity and tumor growth, the study was extended to HCT116 cells, a CRC cell line that also has oncogenic KRAS and an epithelial morphology. HCT116 cells KO for oncogenic KRAS were transfected with the different oncogenic KRAS phosphomutants. Similar to DLD-1 cells, the only clones that were able to form polarized compact organoid-like structures in 3D (analyzed either by phase contrast microscopy or immunofluorescence) were the ones expressing oncogenic KRAS-**S**181 (Supplementary Fig. S5a). Changes of HNFG4 and Neo1 expression observed in the DLD-1 clones, were confirmed in HCT116 cell line (Supplementary Fig. S5b). In contrast, α-E-catenin did not follow the same expression pattern in HCT116 cells than in DLD-1 cells, suggesting that the reduced expression of this protein observed in DLD-1 cells might be a consequence of lack of cell polarization more than the primary cause (Supplementary Fig. S5b). Interestingly, tumor grow upon subcutaneous injection of these cells in mice was also reduced in clones expressing oncogenic KRAS-S181A and KRAS-S181D, compared to the clone expressing the oncogenic KRAS-S181, which is the only one that can be subjected to the phosphorylation-dephosphorylation cycle (Supplementary Fig. S5c).

Finally, we analyzed if expression of higher levels of oncogenic KRAS could revert the decreased tumor growth observed in cells expressing either non-phosphorylatable or phosphomimetic oncogenic KRAS. As shown in Supplementary Fig. S6a, and in agreement with our previous published data[18], DLD-1 cells with high overexpression of oncogenic KRAS-S181**A** had highly impaired the ability to produce subcutaneous tumors. Interestingly, now we show that (in contrast that what occurs in fibroblasts) this ability was also impaired in epithelial cells overexpressing high levels of oncogenic KRAS-S181**D** (Supplementary Fig. S6a). Remarkably, this occurs independently that, in agreement with our previously published data, in 2D-serum restricted conditions, phosphomimetic mutants grew better than non-phosphorylatable mutants (Supplementary Fig. S6b). Thus, suggesting that, independently of the levels of oncogenic KRAS expression, phospho/dephosphorylation cycle of KRAS is essential to support tumor growth, but not growth in 2D cultures. Interestingly, the clones overexpressing phospho/dephosphorylatable oncogenic KRAS were again the only ones

showing some capacity to form polarized organoid-like structures when grown in Matrigel (Supplementary Fig. S6c).

KRAS phosphorylation/dephosphorylation gene expression signature in human colorectal tumors

To analyze the relevance of KRAS phosphorylation status in human CRC development, the expression of genes belonging to the KRAS-S181**A** signature (differentially expressed between oncogenic KRAS-S181**A** and KRAS-**S**181) and genes belonging to the KRAS-S181**D** signature (differentially expressed between oncogenic KRAS-S181**D** and KRAS-**S**181) was examined in a public data set of CRC samples (GSE39582)[33]. Firstly, in general, a positive correlation was observed in the tumors when comparing separately genes upregulated or downregulated belonging to the same signature (either KRAS-S181**A** or KRAS-S181**D**), while a negative correlation was observed when comparing upregulated and repressed genes within a signature (Fig. 6a). Importantly, a negative correlation was observed when comparing KRAS-S181**A** versus KRAS-S181**D** signatures. All this supported the hypothesis that these genes are co-regulated by an upstream event that is most probably dependent on KRAS phosphorylation status. Secondly, when analyzing in the same public cohort gene expression in normal tissue compared to tumor samples, we noticed that gene expression profiles of the tumors were more similar to the KRAS phosphorylation signature than to the non-phosphorylated one (Fig. 6b). Finally, patients with tumors overexpressing *NEO1* (overexpressed in KRAS-S181**A** vs -**S**181) or with tumors with low levels of *SERPINE1* (downregulated in KRAS-S181**A** vs -**S**181) had longer DFS, while patients with tumors with low expression of *HNG4G* (downregulated in KRAS-S181**D** vs –**S**181) or high expression of *ID4* (overexpressed in KRAS-S181**D** vs –**S**181) had a shorter DFS (Fig. 6c).

Discussion

Data presented here indicate that modification of the Ser181 phosphorylation status of oncogenic KRAS in CRC cells strongly impacts on the behavior of these cells: the presence of a phospho/dephosphorylatable residue at position 181 in oncogenic KRAS is essential for cell polarization and aggregation and for facilitating subcutaneous tumor growth; and, cells expressing a non-phosphorylatable or a phosphomimetic amino acid at this position show differential expression of genes with a prominent role in oncogenesis.

The role of phosphorylation of Ser181 in the HVR of KRAS is still controversial. The studies performed to date have mainly been done in non-transformed cell lines as a model, and so what has been analyzed is the contribution of S181 phosphorylation in initial cell transformation[18,20,34]. In the present work we used DLD-1 cells, which are oncogenic KRAS-dependent and have been shown to be a good model for the study of CRC[35,36]. This has allowed us to investigate the role of oncogenic KRAS phosphorylation in maintaining the tumoral properties of cancer cells. An important point of our research is that we exogenously expressed diverse oncogenic KRAS-**S**181 phosphomutants in a modified DLD-1 cell line with a deletion of the endogenous oncogenic KRAS allele (DLD-1 KO), so the endogenous oncogene did not mask the impact of the exogenous phosphomutants. Furthermore, in contrast to our previous study[18], for the main part of the current work, we chose cell clones expressing levels of exogenous oncogenic KRAS similar to those of endogenous WT KRAS, so avoiding possible additional effects due only to oncogenic KRAS overexpression, such as the induction of a mesenchymal phenotype.

Important for our work is that all phosphomutant constructs produced functional oncogenic KRAS proteins, since all recovered the growth of DLD-1 KO cells at serum-starving conditions or in soft agar. This also indicated that the signaling pathways activated by KRAS that allow cells to survive under those conditions are independent of the phosphorylation status of KRAS. Accordingly, a similar impact of all phosphomutants was observed on the last effectors of the main KRAS signaling pathways c-RAF/MEK/ERK and PI3K/AKT.

Although no significant differences were perceived regarding in vitro cell growth, major changes in cellular aggregation and organization were observed between cells expressing the different oncogenic KRAS phosphomutants, the differences being more evident in cells grown in Matrigel. Cells expressing a phospho/dephosphorylatable oncogenic KRAS were the only ones able to form glandular-like structures with polarized cells. This was also observed in HCT116 cells and in DLD-1 cells with overexpression of oncogenic KRAS. One could argue that the mutation of serine to aspartic acid does not properly mimic phosphorylation, but this is unlikely to be the case, since we find a high number of genes differentially expressed between oncogenic KRAS-S181**A** and -S181**D** cells and in all previous publications a different phenotype was observed between cells expressing these phosphophomutants [6,18–20]. Additionally, S181D mutant had a reduced binding to CaM indicating that, at least in this aspect, it was mimicking KRAS phosphorylation. Thus, we hypothesize that the presence of both phosphorylated and dephosphorylated oncogenic KRAS is essential to achieve cell polarity. Interestingly, atypical PKC activity located specifically in the apical domain of epithelial cells is required for proper maintenance of cell polarization[37]. Accordingly, phosphorylated KRAS could also be located in the apical domain and dephosphorylated KRAS in the basolateral domain participating in cell polarization (Supplementary Fig. 7). Lack of cell aggregation and polarization in both oncogenic KRAS-S181**A** and -S181**D**-expressing DLD-1 clones correlated with a reduced expression of *CTNNA1*, which codes for α-E-catenin. Since α-E-catenin facilitates actin attachments at the adherent junctions[38], the lack of α-E-catenin may contribute to the loss of intercellular adhesion. But, because the same pattern of expression of α-E-catenin was not observed in HCT116 cells, decreased levels of this protein in DLD-1 cells may be a consequence and not the primary cause of their inability to organize a well-polarized epithelium in Matrigel.

An important conclusion of the transcriptomic analysis is that the phosphorylation status of KRAS at Ser181 modulates the expression of specific genes in these CRC cells. Besides, it can

be stated that at least a proportion of oncogenic KRAS is being phosphorylated, which we have indirectly confirmed by CaM pull-down.

Gene expression differences between oncogenic KRAS-**S**181 and KRAS-S181**A** cells were mainly found in genes involved in cell migration, invasion and metastases[30,31], indicating that the cells expressing the non-phosphorylatable oncogenic KRAS might have low invasion capacity. These gene expression changes were corroborated in another CRC cell line, SW480, in which we introduced a S181**A** mutation in one of the oncogenic KRAS alleles. Most interestingly, these mutant cells displayed less ability to invade. Although further experiments are needed, from our results we suggest that oncogenic KRAS phosphorylation enhances cell invasion.

Additionally, the specific differences in gene expression induced by the phosphomimetic mutant, imply that phosphorylation of KRAS promotes an undifferentiated cellular state related to cancer progression. The reduced expression of genes such as *HNF4G*[27], *HEPH*, *UGT1A* and *MUC13*[24–26], and the GSEA data associate KRAS phosphorylation with pluripotency[28].

Notably, expression correlation analysis, in a cohort of human CRC, between genes belonging to the different signatures strongly supports the hypothesis that gene expression is also regulated by KRAS phosphorylation in human tumors.

While all cells expressing the different phosphomutants of oncogenic KRAS were able to grow in 2D and 3D cultures, subcutaneous tumor growth, independently of the levels of expression of the phosphomutant, was strongly impaired in KRAS-S181**A** and in KRAS-S181**D**-expressing cells. Results obtained with the non-phosphorylatable mutant agreed completely with our previous observations [18], but based on the gene expression data and in 2D culture results, it was surprising that the phosphomimetic mutant did not support tumor growth. Interestingly, lack of tumor growth correlated (independently of the levels of oncogene expression) with the inability to form polarized organoid-like structures in Matrigel. The poorly differentiated histological morphology and the lack of a well-organized perivascular organization observed in oncogenic

KRAS-S181**D** and KRAS-S181**A** tumors may reflect the 3D culture findings (Supplementary Fig. 7) and may preclude tumor nutrition and oxygenation (in agreement with the observed CA-IX expression), and consequently tumor growth. We propose that, as was the case with Matrigel, a phosphorylation/dephosphorylation cycle is necessary to polarize and organize the cells around blood vessels. Interestingly, cell polarity in CRCs is disrupted but not completely lost[39]. Thus, a selective pressure to maintain certain cell polarity may exist in colorectal tumors. Accordingly, α-E-catenin has an essential role in intestinal adenoma formation[40] and together with other components of the cadherin complex is considered an obligatory haploinsufficient tumor suppressor in intestinal neoplasia[41]. The need of cell polarization for CRC tumor growth, may explain the differences observed regarding the ability of mouse fibroblast transfected with oncogenic KRAS-S181**D** to generate subcutaneous tumors[18]. Based on the findings presented here one might think that inducing either complete KRAS phosphorylation or dephosphorylation would be a good therapeutic strategy: both PKC inhibitors and activators have been shown to reduce tumor growth induced by oncogenic KRAS[18,42]. Nevertheless, present data related to cell invasion and differentiation, together with our previous observations in mouse fibroblasts[6,12,18], suggest that inhibiting KRAS phosphorylation would be safer. Most importantly, analysis of the public data indicates that gene expression in human CRC is more similar to the phosphomimetic than to the non-phosphorylatable oncogenic KRAS signature, supporting the hypothesis that phosphorylation is important for human CRC development, and that consequently its inhibition would be a good therapeutic strategy.

We conclude that CRC cells depend on KRAS phosphorylation cycle at Ser181 to maintain their tumorigenic properties. Specific interference with this modification or with its downstream signaling may be an appropriate therapy.

Materials and Methods

Cell lines and culture. DLD-1 ($KRAS^{WT/G13D}$) (clone V15, #HD PAR-086) and HCT116 ($KRAS^{WT/G13D}$) (#HD PAR-007) colorectal adenocarcinoma cell lines, and DLD-1 and HCT116 knockouts of mutant KRAS allele, DLD-1 KO ($KRAS^{WT/-}$) (clone D-WT7, #HD105-002) and HCT116 KO ($KRAS^{WT/-}$) (clone HAF1 (v154), #HD 104-008) were obtained from Horizon Discovery Ltd. (Cambridge, UK). DLD-1 KO and HCT116 KO mutant clones stably expressing HA-KRAS-G12V-**S**181, HA-KRAS-G12V-S181**A**, or HA-KRAS-G12V-S181**D** were generated by transfecting DLD-1 KO and HCT116 KO cells with the specific HA-KRAS-G12V plasmids as indicated in Supplementary Methods. SW480 cells with one oncogenic KRAS allele containing the S181**A** mutation was generated by single guide wild-type Cas9-based CRISPR technology [43] (see details in supplementary methods). DLD-1 and DLD-1 KO cells were grown in DMEM-HAM's F12 (1:1), and SW480 in DMEM. In all cases medium was supplemented as previously described[18]. Cells were tested one per month for mycoplasma contamination.

Cell growth and Proliferation assays, Cell invasion Assay, and Sample lysis and Western blotting are detailed in Supplementary Methods and supplementary table S2

3-Dimensional (3D) cell culture. 3D on-top Matrigel assay was performed as in ref. [44]. For details and also for soft agar colony formation assay see Supplementary Methods.

Immunofluorescence for 3D cell culture. Organoid-like structures of growing cells were fixed following option C of the protocol for whole-culture fixation[44]**.** See detailed in Supplementary Methods.

CaM-Sepharose Pull-down Assays were performed as previously described[9].

Tumor generation in mice. Subcutaneous tumors were generated as previously described[18]. See details in Supplementary Methods**.**

All mouse experiments were performed in accordance with protocols approved by the Animal Care and Use Committee of ICO-IDIBELL Hospitalet de Llobregat (Barcelona, Spain). For tumor histology and histochemistry see Supplementary Methods. Antibodies and reagents used are listed in Supplementary Table S3.

Microarrays and gene expression analysis. See Supplementary Methods and references[29,45–50] and Supplementary Table S4

Statistical Analysis. Statistical analyses were performed with GraphPad Prism 8.1. Data shown represent the mean ± SEM or SD (as indicated in figure legends) of three or four independent experiments. Significant differences were assessed using one-way ANOVA with Tukey's or Dunnett's Multiple Comparisons Tests; and considered when $P<0.05$.

Data and code availability. The datasets generated during the current study are available in the GEO database repository: https://www.ncbi.nlm.nih.gov/geo/query/acc.cgi?acc=GSE176276

Acknowledgements

We thank the personnel of the Advanced Microscopy Unit of CCiT-UB (Campus Clinic) for the help in setting up image acquisition and analysis.

This work was supported by grants from the Ministerio de Economia y Competitividad and co-funded by FEDER funds –a way to build Europe- (SAF2016-76239-R and PID2019-105483RB-I00 to NA, SAF2015-68016-R to GC), CIBERONC and the Governement of Catalonia (grants 2017SGR1282 and PERIS SLT002/16/0037), and from Instituto de Salud Carlos III (grant PI17/01304 to MC); a FPU fellowship from Ministerio de Educación, Cultura y Deporte for DC, a FI fellowship from Generalitat de Catalunya for NP, and a Predoc-UB from

University of Barcelona to BA; CR is supported by the Serra Húnter Program (Generalitat de Catalunya).

Competing Interests

Authors declare there is not any competing financial interests in relation to the work described.

Supplementary information is available at Oncogene's website.

References

1 Malumbres M, Barbacid M. RAS oncogenes: the first 30 years. *Nat Rev Cancer* 2003; **3**: 459–65.

2 Bourne HR, Sanders DA, McCormick F. The GTPase superfamily: conserved structure and molecular mechanism. *Nature* 1991; **349**: 117–127.

3 Hancock JF, Magee AI, Childs JE, Marshall CJ. All ras proteins are polyisoprenylated but only some are palmitoylated. *Cell* 1989; **57**: 1167–77.

4 Simanshu DK, Nissley D V., McCormick F. RAS Proteins and Their Regulators in Human Disease. *Cell* 2017; **170**: 17–33.

5 Chandra A, Grecco HE, Pisupati V, Perera D, Cassidy L, Skoulidis F *et al.* The GDI-like solubilizing factor PDEδ sustains the spatial organization and signalling of Ras family proteins. *Nat Cell Biol* 2012; **14**: 148–58.

6 Alvarez-Moya B, López-Alcalá C, Drosten M, Bachs O, Agell N. K-Ras4B phosphorylation at Ser181 is inhibited by calmodulin and modulates K-Ras activity and function. *Oncogene* 2010; **29**: 5911–22.

7 Stephen AG, Esposito D, Bagni RG, McCormick F. Dragging ras back in the ring. *Cancer Cell* 2014; **25**: 272–281.

8 Shalom-Feuerstein R, Plowman SJ, Rotblat B, Ariotti N, Tian T, Hancock JF *et al.* K-ras nanoclustering is subverted by overexpression of the scaffold protein galectin-3. *Cancer Res* 2008; **68**: 6608–16.

9 Lopez-Alcalá C, Alvarez-Moya B, Villalonga P, Calvo M, Bachs O, Agell N. Identification of essential interacting elements in K-Ras/calmodulin binding and its role in K-Ras localization. *J Biol Chem* 2008; **283**: 10621–31.

10 Garrido E, Lázaro J, Jaumot M, Agell N, Rubio-Martinez J. Modeling and subtleties of K-Ras and Calmodulin interaction. *PLoS Comput Biol* 2018; **14**: 1–19.

11 Villalonga P, López-Alcalá C, Bosch M, Chiloeches A, Rocamora N, Gil J *et al.* Calmodulin binds to K-Ras, but not to H- or N-Ras, and modulates its downstream signaling. *Mol Cell Biol* 2001; **21**: 7345–54.

12 Barceló C, Etchin J, Mansour MR, Sanda T, Ginesta MM, Sanchez-Arévalo Lobo VJ *et al.* Ribonucleoprotein HNRNPA2B1 interacts with and regulates oncogenic KRAS in pancreatic ductal adenocarcinoma cells. *Gastroenterology* 2014; **147**: 882-892.e8.

13 Inder KL, Lau C, Loo D, Chaudhary N, Goodall A, Martin S *et al.* Nucleophosmin and nucleolin regulate K-Ras plasma membrane interactions and MAPK signal transduction. *J Biol Chem* 2009; **284**: 28410–9.

14 Lee S, Jeong W, Cho Y, Cha P, Yoon J, Ro EJ *et al.* β□Catenin□RAS interaction serves as a molecular switch for RAS degradation via GSK3β. *EMBO Rep* 2018; : e46060.

15 Villalonga P, López-Alcalá C, Chiloeches A, Gil J, Marais R, Bachs O *et al.* Calmodulin prevents activation of Ras by PKC in 3T3 fibroblasts. *J Biol Chem* 2002; **277**: 37929–37935.

16 Barceló C, Paco N, Beckett AJ, Alvarez-Moya B, Garrido E, Gelabert M *et al.* Oncogenic K-ras segregates at spatially distinct plasma membrane signaling platforms according to its phosphorylation status. *J Cell Sci* 2013; **126**: 4553–9.

17 Yang MH, Nickerson S, Kim ET, Liot C, Laurent G, Spang R *et al.* Regulation of RAS oncogenicity by acetylation. *Proc Natl Acad Sci U S A* 2012; **109**: 10843–8.

18 Barcelo C, Paco N, Morell M, Alvarez-Moya B, Bota-Rabassedas N, Jaumot M *et al.* Phosphorylation at Ser-181 of oncogenic KRAS is required for tumor growth. *Cancer Res* 2014; **74**: 1190–1199.

19 Wang MT, Holderfield M, Galeas J, Delrosario R, To MD, Balmain A *et al.* K-Ras Promotes Tumorigenicity through Suppression of Non-canonical Wnt Signaling. *Cell* 2015; **163**: 1237–1251.

20 Bivona TG, Quatela SE, Bodemann BO, Ahearn IM, Soskis MJ, Mor A *et al.* PKC regulates a farnesyl-electrostatic switch on K-Ras that promotes its association with Bcl-XL on mitochondria and induces apoptosis. *Mol Cell* 2006; **21**: 481–93.

21 Sasaki AT, Carracedo A, Locasale JW, Anastasiou D, Takeuchi K, Kahoud ER *et al.* Ubiquitination of K-Ras enhances activation and facilitates binding to select downstream effectors. *Sci Signal* 2011; **4**: ra13.

22 Vartanian S, Bentley C, Brauer MJ, Li L, Shirasawa S, Sasazuki T *et al.* Identification of mutant K-Ras-dependent phenotypes using a panel of isogenic cell lines. *J Biol Chem* 2013; **288**: 2403–2413.

23 Shirasawa S, Furuse M, Yokoyama N, Sasazuki T. Altered growth of human colon cancer cell lines disrupted at activated Ki-ras. *Science (80-)* 1993; **260**: 85 LP – 88.

24 Brookes MJ, Hughes S, Turner FE, Reynolds G, Sharma N, Ismail T *et al.* Modulation of iron transport proteins in human colorectal carcinogenesis. *Gut* 2006; **55**: 1449–1460.

25 Hu DG, Mackenzie PI, McKinnon RA, Meech R. Genetic polymorphisms of human UDP-glucuronosyltransferase (UGT) genes and cancer risk. *Drug Metab Rev* 2016; **48**: 47–69.

26 Maher DM, Gupta BK, Nagata S, Jaggi M, Chauhan SC. Mucin 13: Structure, function, and potential roles in cancer pathogenesis. *Mol Cancer Res* 2011; **9**: 531–537.

27 Lindeboom RG, van Voorthuijsen L, Oost KC, Rodríguez□Colman MJ, Luna□Velez M V, Furlan C *et al.* Integrative multi□omics analysis of intestinal organoid differentiation. *Mol Syst Biol* 2018; **14**: e8227.

28 Santiago L, Daniels G, Wang D, Deng M, Lee P. Wnt signaling pathway protein LEF1 in cancer, as a biomarker for prognosis and a target for treatment. *Am J Cancer Res* 2017; **7**: 1389–1406.

29 Hou Z, Guo K, Sun X, Hu F, Chen Q, Luo X *et al.* TRIB2 functions as novel oncogene

in colorectal cancer by blocking cellular senescence through AP4/p21 signaling. *Mol Cancer* 2018; **17**: 1–15.

30 Yamamoto H, Iku S, Adachi Y, Imsumran A, Taniguchi H, Nosho K *et al.* Association of trypsin expression with tumour progression and matrilysin expression in human colorectal cancer. *J Pathol* 2003; **199**: 176–184.

31 Li S, Wei X, He J, Tian X, Yuan S, Sun L. Plasminogen activator inhibitor-1 in cancer research. *Biomed Pharmacother* 2018; **105**: 83–94.

32 Chaturvedi V, Fournier-Level A, Cooper HM, Murray MJ. Loss of Neogenin1 in human colorectal carcinoma cells causes a partial EMT and wound-healing response. *Sci Rep* 2019; **9**: 1–15.

33 Marisa L, de Reyniès A, Duval A, Selves J, Gaub MP, Vescovo L *et al.* Gene Expression Classification of Colon Cancer into Molecular Subtypes: Characterization, Validation, and Prognostic Value. *PLoS Med* 2013; **10**: e1001453.

34 Yin N, Liu Y, Khoor A, Wang X, Thompson EA, Leitges M *et al.* Protein Kinase Cι and Wnt/β-Catenin Signaling: Alternative Pathways to Kras/Trp53-Driven Lung Adenocarcinoma. *Cancer Cell* 2019; **36**: 156-167.e7.

35 Mouradov D, Sloggett C, Jorissen RN, Love CG, Li S, Burgess AW *et al.* Colorectal cancer cell lines are representative models of the main molecular subtypes of primary cancer. *Cancer Res* 2014; **74**: 3238–3247.

36 Berg KCG, Eide PW, Eilertsen IA, Johannessen B, Bruun J, Danielsen SA *et al.* Multi-omics of 34 colorectal cancer cell lines - a resource for biomedical studies. *Mol Cancer* 2017; **16**: 1–16.

37 Román-Fernández A, Bryant DM. Complex Polarity: Building Multicellular Tissues Through Apical Membrane Traffic. *Traffic* 2016; **17**: 1244–1261.

38 Maiden SL, Hardin J. The secret life of α-catenin: Moonlighting in morphogenesis. *J*

Cell Biol 2011; **195**: 543–552.

39 Compton CC. Colorectal carcinoma: Diagnostic, prognostic, and molecular features. *Mod Pathol* 2003; **16**: 376–388.

40 Shibata H, Takano H, Ito M, Shioya H, Hirota M, Matsumoto H *et al.* Alpha-Catenin is essential in intestinal adenoma formation. *Proc Natl Acad Sci* 2007; **104**: 18199–18204.

41 Short SP, Kondo J, Smalley-Freed WG, Takeda H, Dohn MR, Powell AE *et al.* p120-Catenin is an obligate haploinsufficient tumor suppressor in intestinal neoplasia. *J Clin Invest* 2017; **127**: 4462–4476.

42 Elia AEH, Wang DC, Willis NA, Boardman AP, Hajdu I, Adeyemi RO *et al.* RFWD3-Dependent Ubiquitination of RPA Regulates Repair at Stalled Replication Forks. *Mol Cell* 2015; **60**: 280–293.

43 Ran FA, Hsu PD, Wright J, Agarwala V, Scott DA, Zhang F. Genome engineering using the CRISPR-Cas9 system. *Nat Protoc* 2013; **8**: 2281–2308.

44 Lee GY, Kenny PA, Lee EH, Bissell MJ. Three-dimensional culture models of normal and malignant breast epithelial cells. *Nat Methods* 2007; **4**: 359–365.

45 Gogarten SM, Bhangale T, Conomos MP, Laurie CA, McHugh CP, Painter I *et al.* GWASTools: An R/Bioconductor package for quality control and analysis of genome-wide association studies. *Bioinformatics* 2012; **28**: 3329–3331.

46 Subramanian A, Tamayo P, Mootha VK, Mukherjee S, Ebert BL, Gillette MA *et al.* Gene set enrichment analysis: A knowledge-based approach for interpreting genome-wide expression profiles. *Proc Natl Acad Sci U S A* 2005; **102**: 15545–50.

47 Cortazar AR, Torrano V, Martín-Martín N, Caro-Maldonado A, Camacho L, Hermanova I *et al.* Cancertool: A visualization and representation interface to exploit cancer datasets. *Cancer Res* 2018; **78**: 6320–6328.

48 Livak KJ, Schmittgen TD. Analysis of relative gene expression data using real-time

quantitative PCR and the 2-ΔΔCT method. *Methods* 2001; **25**: 402–8.

49 Humphries BA, Buschhaus JM, Chen YC, Haley HR, Qyli T, Chiang B *et al.* Plasminogen activator inhibitor 1 (PAI1) promotes actin cytoskeleton reorganization and glycolytic metabolism in triple-negative breast cancer. *Mol Cancer Res* 2019; **17**: 1142–1154.

50 Wang J, Zhang J, Xu L, Zheng Y, Ling D, Yang Z. Expression of HNF4G and its potential functions in lung cancer. *Oncotarget* 2018; **9**: 18018–18028.

Figure legends

Fig. 1 Stable expression of oncogenic KRAS phosphomutants induce differential cell morphology. a WB analysis showing the clones of DLD-1 KO ($KRAS^{WT/-}$) with an exogenous expression of KRAS-G12V-S181 (**S**181), KRAS-G12V-S181A (S181**A**) and KRAS-G12V-S181D (S181**D**) similar to the endogenous level of KRAS (numbers indicate different clones) (upper panel). Phase-contrast images of KRAS phosphomutants cell clones. All scale bars, 50 μm (bottom panel). **b** 5 x 10^3 DLD-1 KO ($KRAS^{WT/-}$) cells stably expressing either KRAS-G12V-**S**181, -S181**A**, or -S181**D** were cultured under serum-limiting (0.1% FBS) conditions for 48 hours to evaluate cell survival by MTT. A cell viability ratio was obtained for each clone. Mean ± SEM of four independent experiments is shown. Significant differences were assessed using one-way ANOVA and Dunnett's Multiple Comparisons Tests compared to DLD-1 KO (*p-value<0.05, **p-value<0.01, ***p-value<0.001, ****p-value<0.0001). **c** DLD-1 KO ($KRAS^{WT/-}$) cells expressing KRAS-G12V phosphomutants were cultured in absence of serum (0% FBS) for 24 hours and total lysates from the different cell clones were analyzed by WB to detect the indicated proteins. Lamin B and Gap120 were used as loading controls of phosphoproteins. *Gap120 was used as loading controls of total proteins.

Fig. 2 Status of oncogenic KRAS phosphorylation at Ser181 has an impact in genes expression. a Average linkage WPGMA Clustering of proves and clones that had a significantly different expression (FDR<0.01 (False Discovery Rate)) in at least one of the conditions (**S**181; S181**A** or S181**D**)**.** Intensities (Log2) were normalized for each gene. **b** Differentially expressed probes were pooled in genes to determine the number of genes differentially expressed. Number of genes (upper graph) and Venn diagram (lower graph) of differentially expressed (FDR<0.05 and a FC>2 (Fold Change)) between the phosphomutant groups. **c** Volcano plot showing genes differentially expressed when comparing S181**D** (upper graph) or S181**A** (lower graph) with **S**181 expressing cells. Genes with an FDR<0.05 and a FC>2 are colored: red upregulated and green downregulated. The name of genes of interest is indicated. **d** RNA extraction from DLD-1 KO ($KRAS^{WT/-}$) cells stably expressing KRAS-G12V-

S181, -S181**A** or -S181**D** was carried out and cDNA was obtained from 1µg of total RNA. Real Time qPCR was performed. The normalized expression of *CTNNA1*, *SERPINE1*, *PRSS2*, *HNF4G* and *TRIB2* is presented relative to the expression in KRAS-G12V-**S**181 phosphomutant. Data shown represent the mean ± SEM of three independent experiments (**S**181, S181**A** and S181**D** indicate the average of three different KRAS-G12V-**S**181, -S181**A** or -S181**D** cell clones). Significant differences were assessed using one-way ANOVA and Dunnett's Multiple Comparisons Tests compared to **S**181 (*p-value<0.05, **p-value<0.01, ***p-value<0.001, ****p-value<0.0001). **e** GSEA plot showing enrichment of the indicated gene set in the expression profile of S181**D** versus **S**181 and S181**A** versus S181**D** cells. NES, normalized enrichment score; P, p-value.

Fig. 3 Oncogenic KRAS phosphorylation/dephosphorylation cycle at Ser181 is necessary to induce an epithelial polarized structure. a Cell extracts from DLD-1 KO ($KRAS^{WT/-}$) cells stably expressing KRAS phosphomutants cultured in 2D were immunoblotted using the indicated antibodies. CDK4 and lamin B were used as loading controls**. b** 2.5 x 10^4 DLD-1 KO ($KRAS^{WT/-}$) cells stably expressing either KRAS-G12V-**S**181, -S181**A**, or -S181**D** were cultured on top of a thin basement membrane matrix (Matrigel) overlaid with a dilute solution of this basement membrane matrix (3D on-top Matrigel assay). Representative phase-contrast images of phosphomutants cells grown for seven days are shown. All scale bars, 50 µm. **c** After seven days, colonies were immunostained to detect E-cadherin (adherent junctions, green), integrin α-6 (basement membrane marker, green), α-E-catenin (cell adhesion, green) and polymerized actin was detected with phalloidin (apical cell marker, red). Nuclei were counterstained with DAPI (blue). A representative image of one of each phosphomutants is shown. All scale bars, 10 µm.

Fig. 4 Oncogenic KRAS phosphorylation/dephosphorylation cycle at Ser181 regulates cell invasive capacity. SW480 cells (**S**181) and different clones of CRISPR modified SW480 cells with one KRAS allele with S181**A** mutation (named as S181**A** followed by the number of the

667 clone) were used. **a** RNA extraction from SW480 cells (**S**181) and SW480 cells with S181**A**
668 mutation was carried out and cDNA was obtained from 1µg of total RNA. Real Time qPCR was
669 performed. The normalized expression of *SERPINE1* and *CTNNA1* is expressed in the graph
670 relative to SW480 cells (**S**181). Data shown represent the mean ± SEM of four independent
671 experiments. Significant differences were assessed using one-way ANOVA and Dunnett's
672 multiple comparisons tests compared to SW480 cell line (**S**181) (*p-value<0.05, **p-
673 value<0.01, ***p-value<0.001, ****p-value<0.0001). # significant differences using unpaired
674 two-tailed t test. **b** Cell extracts from SW480 cells (**S**181) and SW480 cells with S181**A**
675 mutation were immunobloted to detect the indicated proteins. Gap120 and CDK4 were used as
676 loading controls. **c** Cell invasion assay was performed as detailed in methods section**.** The
677 number of invading cells was calculated as the number of cells counted in the lower
678 compartment of Boyden chamber divided by the number of areas counted**.** Data show the
679 invading cell ratio and represent the mean ± SEM of three independent experiments. Significant
680 differences were assessed using one-way ANOVA and Dunnett's Multiple Comparisons Tests
681 compared to SW480 cell line (**S**181) (*p-value<0.05, **p-value<0.01, ***p-value<0.001,
682 ****p-value<0.0001).
683
684 **Fig. 5 Phosphorylation at Ser181 of oncogenic KRAS is necessary for tumor growth.** DLD-
685 1 KO ($KRAS^{WT/-}$) cells stably expressing either KRAS-G12V-**S**181 (clone S3), -S181**A** (clone
686 A1) or –S181**D** (clone D2**)** were injected into each flank of nude mice (each group n=4 tumors).
687 **a** Oncogenic KRAS exogenous protein levels from the different cell clones were analyzed by
688 immunoblot the day of injection into mice. Lamin B was used as loading control. **b** At day 28
689 mice were euthanized, and tumors were dissected and weighed. The weight of excised tumors is
690 showed in the graph (each dot corresponds to a tumor). Mean ± SD of four tumors of each
691 phosphomutant is shown. Significant differences were assessed using one-way ANOVA and
692 Dunnett's Multiple Comparisons Tests comparing to **S**181-derived tumor (*p-value<0.05, **p-
693 value<0.01, ***p-value<0.001, ****p-value<0.0001). **c** Histology of tumors was analyzed by
694 hematoxylin-eosin staining. Slide scan and morphometric analysis were performed. The panels

show from left to right the lowest to highest magnification images. Scale bars of lowest magnification, 200μm. Scale bars of highest magnifications, 50μm. **d-e** Total cell lysates of representative excised tumors were immunoblotted to detect the indicated proteins (numbers indicate different tumors). CDK4, tubulin and Gap120 were used as loading controls **(d)**. Gap120 and *Gap120 were used as loading controls of phospho- and total proteins, respectively **(e).**

Fig. 6 Expression of S181D and S181A signature in human CRC primary tumors and normal colon. a Correlation matrix (Pearson's Coefficient) between the expression of genes belonging to S181**A** and S181**D** signatures analyzed in human CRC primary tumors (GSE39582). We are more restrictive with the S181**D** signature in order to have a similar number of genes in each one. *UGT1A1-10* and *CTNNA1* are excluded from the analysis (the first because is a group of genes and the second because it belongs to both signatures). Correlation is considered if p-value P<0.01 (student T-test). **b** Color-map showing relative expression of genes belonging to S181**A** and S181**D** signatures in CRC human primary tumors (CRC T) versus normal tissue (NT) (GSE39582). Differences were considered if p-value P<0.01. **c** DFS Kaplan-Meyer curves using the same cohort as in (**a**) and (**b**). Each curve represents the percentage (Y-axis) of the population that exhibits recurrence of the disease along time (X-axis, in months) for each indicated quartile.

Authors' contributions

DC and SB contributed equally to this work; DC, SB, NP, MMG, BA and NG-S conducted the experiments and data analysis; CB, MC, JME, MB, CR, GC, MJ and NA conducted data analysis and interpretation; TR-F, GP and CR provided technical set-up and support. MJ and NA designed the study; MJ, DC and NA wrote the manuscript. All authors read and approve the final manuscript.

NA (neusagell@ub.edu) and MJ (mjaumot@ub.edu) are corresponding authors.

722

Figure 1

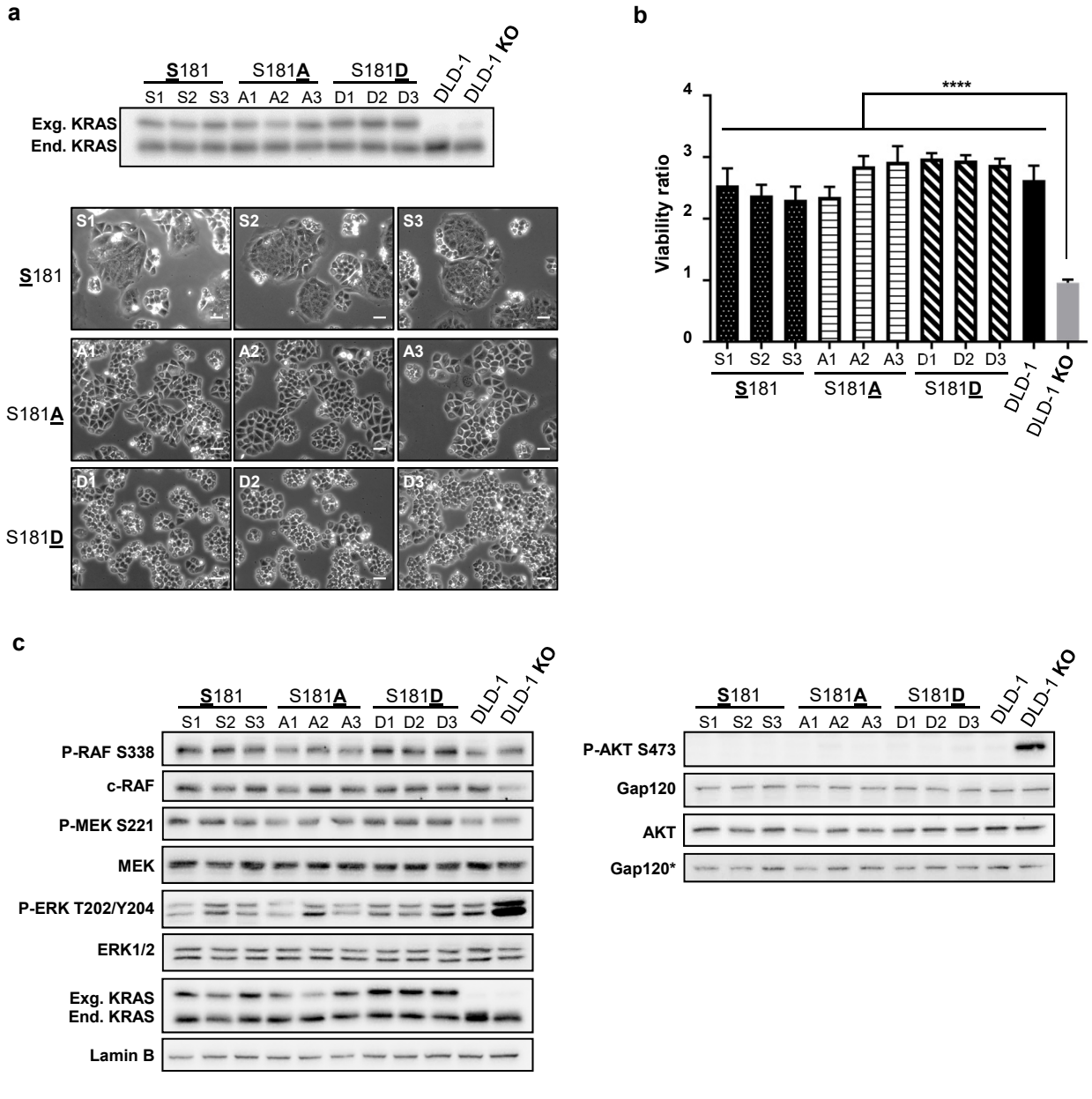
a
S181
S181A
S181D
S1 S2 S3 A1 A2 A3 D1 D2 D3
DLD-1
DLD-1 KO
Exg. KRAS
End. KRAS
S1
S2
S3
A1
A2
A3
D1
D2
D3
b
Viability ratio
****
0
1
2
3
4
c
P-RAF S338
c-RAF
P-MEK S221
MEK
P-ERK T202/Y204
ERK1/2
Exg. KRAS
End. KRAS
Lamin B
P-AKT S473
Gap120
AKT
Gap120*

Figure 2

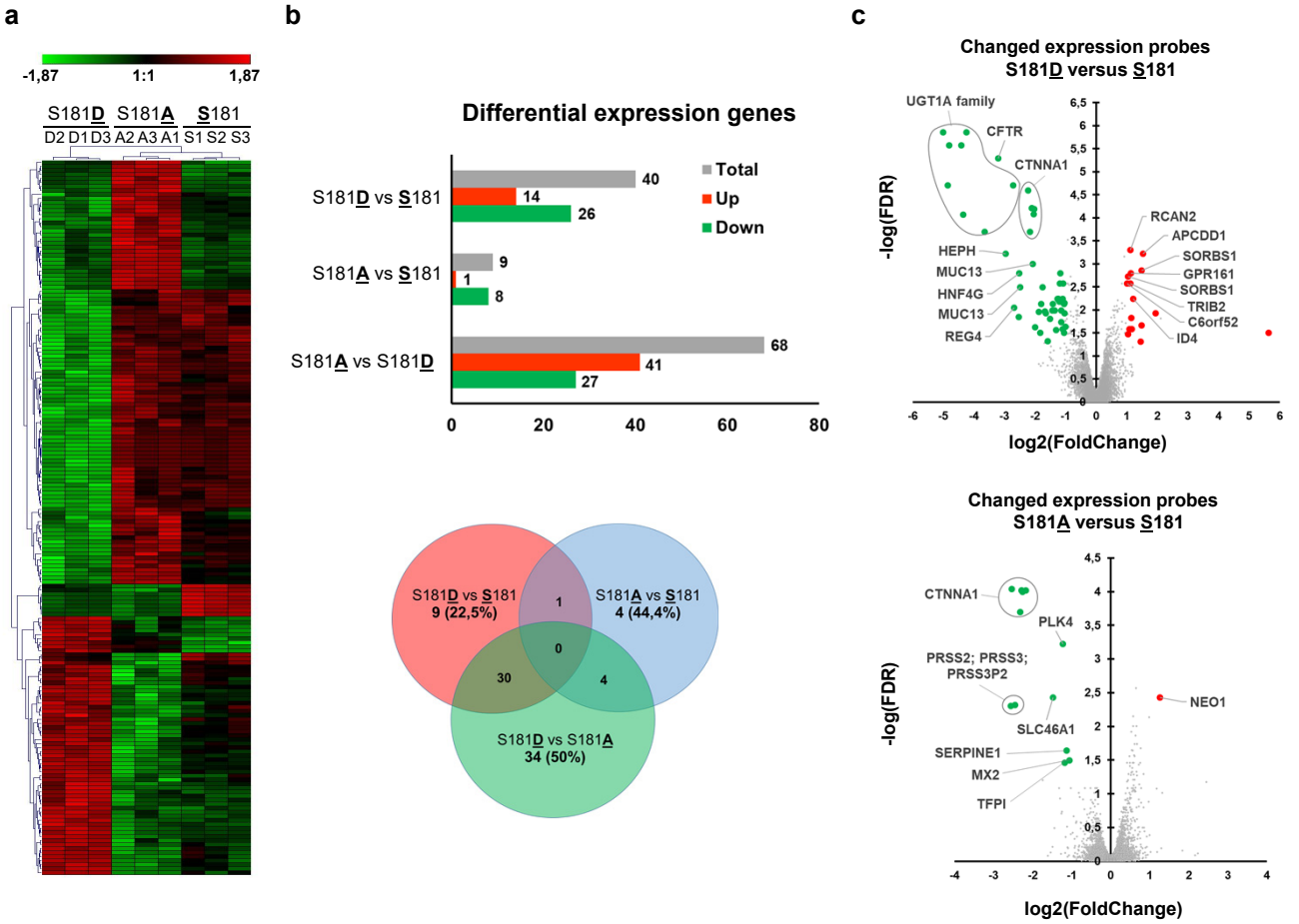
a
-1,87
1:1
1,87
S181D S181A S181
D2 D1 D3 A2 A3 A1 S1 S2 S3
b
Differential expression genes
S181D vs S181
S181A vs S181
S181A vs S181D
Total
Up
Down
40
14
26
9
1
8
68
41
27
0
20
40
60
80
S181D vs S181
9 (22,5%)
S181A vs S181
4 (44,4%)
S181D vs S181A
34 (50%)
1
0
30
4
c
Changed expression probes
S181D versus S181
-log(FDR)
log2(FoldChange)
UGT1A family
CFTR
CTNNA1
HEPH
MUC13
HNF4G
MUC13
REG4
RCAN2
APCDD1
SORBS1
GPR161
SORBS1
TRIB2
C6orf52
ID4
Changed expression probes
S181A versus S181
CTNNA1
PLK4
PRSS2; PRSS3;
PRSS3P2
SLC46A1
SERPINE1
MX2
TFPI
NEO1
d
Relative mRNA level of HNF4G
Relative mRNA level of TRIB2
Relative mRNA level of SERPINE1
Relative mRNA level of PRSS2
Relative mRNA level of CTNNA1
S181
S181A
S181D
e
LEF1-UP signature
Upregulated genes
NES=1,83
P=0,000
LEF1-UP signature
Downregulated genes
NES=-2,81
P=0,000
LEF1-UP signature
Upregulated genes
NES=-1,83
P=0,000
LEF1-UP signature
Downregulated genes
NES=2,23
P=0,000

Figure 3

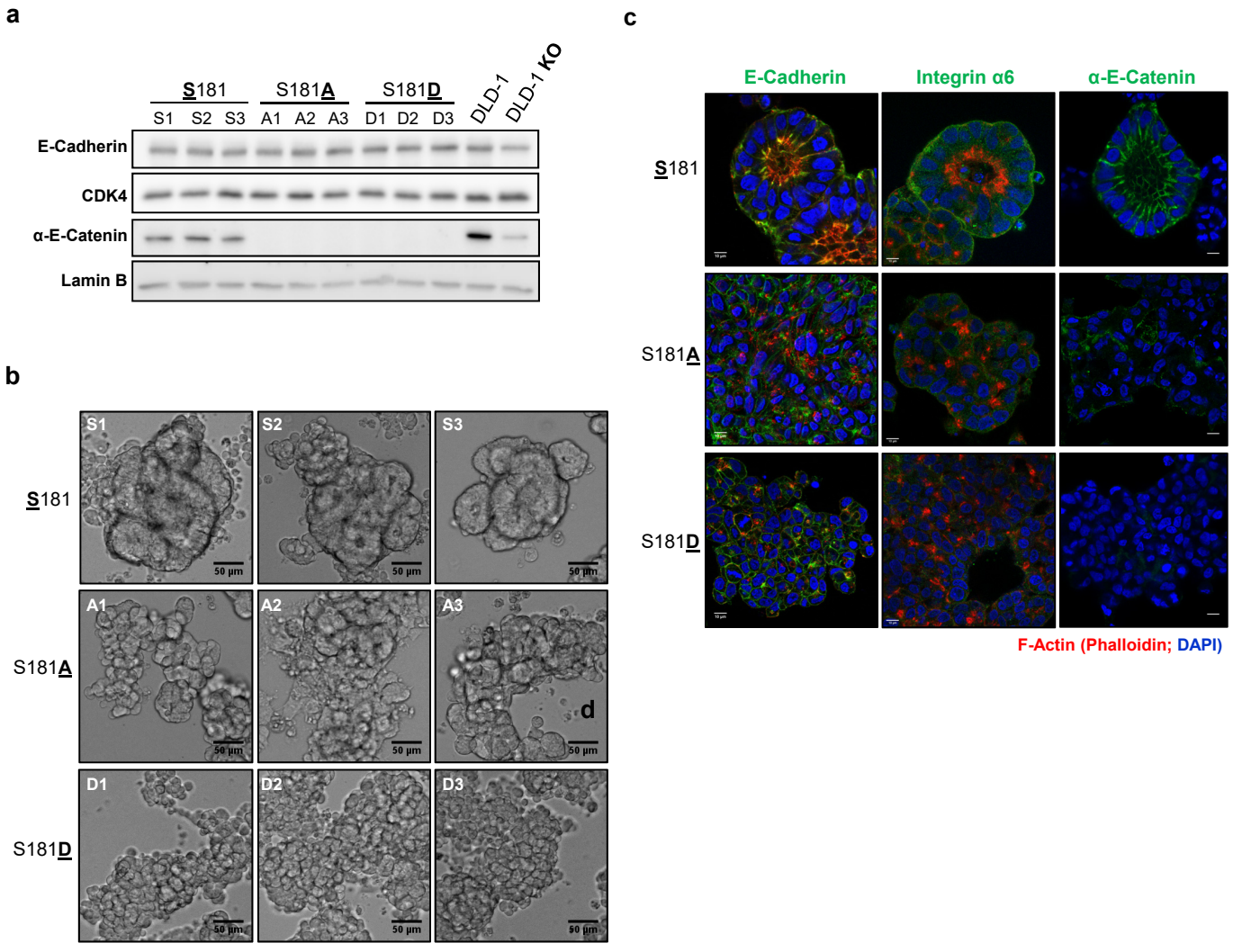
a
S181
S181A
S181D
S1 S2 S3 A1 A2 A3 D1 D2 D3
DLD-1
DLD-1 KO
E-Cadherin
CDK4
α-E-Catenin
Lamin B
b
S181
S181A
S181D
S1
S2
S3
A1
A2
A3
D1
D2
D3
50 μm
c
E-Cadherin
Integrin α6
α-E-Catenin
S181
S181A
S181D
F-Actin (Phalloidin; DAPI)

Figure 4

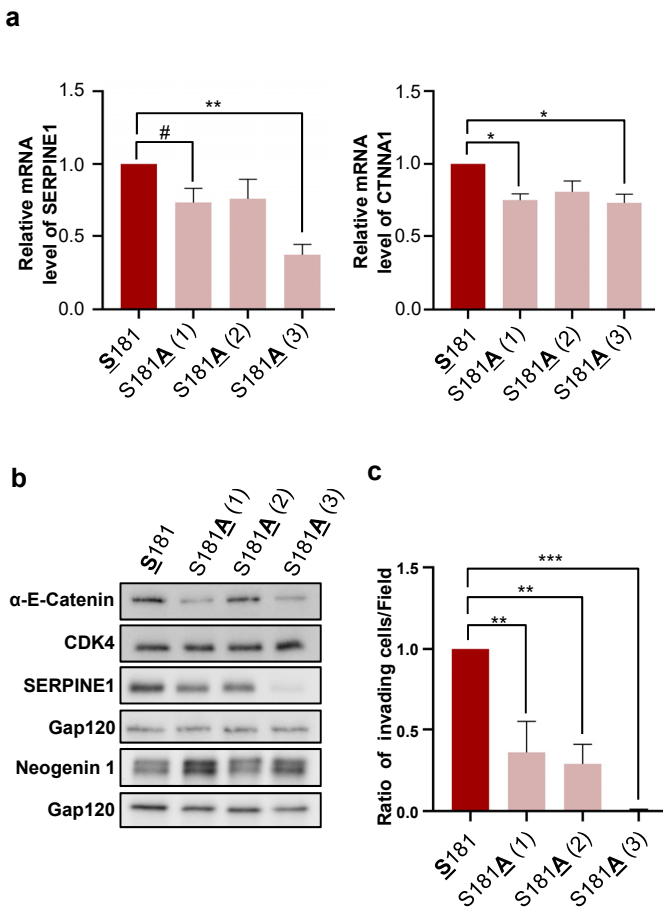
a
Relative mRNA level of SERPINE1
Relative mRNA level of CTNNA1
1.5
1.0
0.5
0.0
**
#
*
*
S181
S181A (1)
S181A (2)
S181A (3)
b
S181
S181A (1)
S181A (2)
S181A (3)
α-E-Catenin
CDK4
SERPINE1
Gap120
Neogenin 1
Gap120
c
Ratio of invading cells/Field
***
**
**

Figure 5

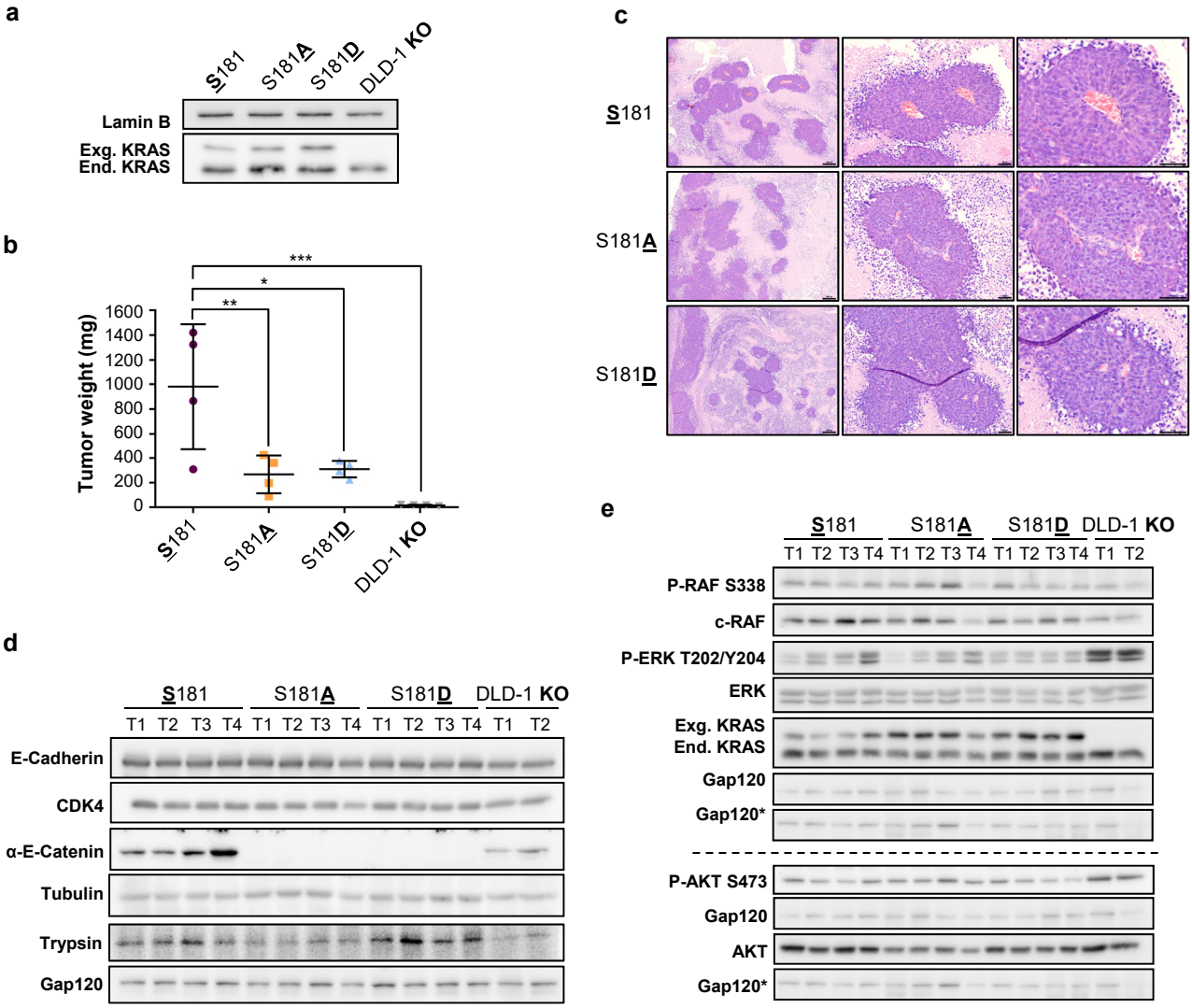
a
S181
S181A
S181D
DLD-1 KO
Lamin B
Exg. KRAS
End. KRAS
b
Tumor weight (mg)
1600
1400
1200
1000
800
600
400
200
0
***
*
**
S181
S181A
S181D
DLD-1 KO
c
S181
S181A
S181D
d
S181
S181A
S181D
DLD-1 KO
T1 T2 T3 T4 T1 T2 T3 T4 T1 T2 T3 T4 T1 T2
E-Cadherin
CDK4
α-E-Catenin
Tubulin
Trypsin
Gap120
e
S181
S181A
S181D
DLD-1 KO
T1 T2 T3 T4 T1 T2 T3 T4 T1 T2 T3 T4 T1 T2
P-RAF S338
c-RAF
P-ERK T202/Y204
ERK
Exg. KRAS
End. KRAS
Gap120
Gap120*
P-AKT S473
Gap120
AKT
Gap120*

Figure 6

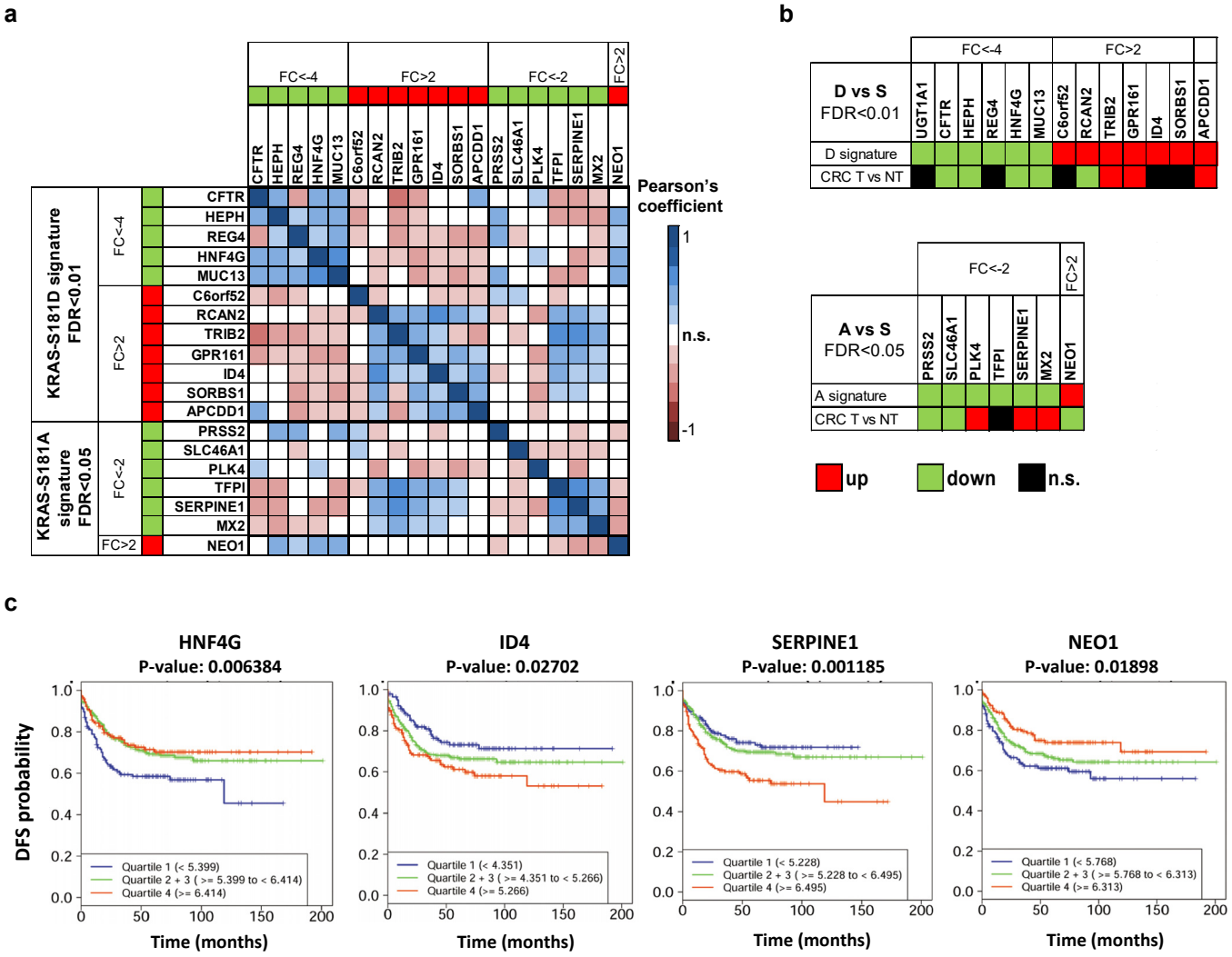
a
FC<-4
FC>2
FC<-2
FC>2
CFTR
HEPH
REG4
HNF4G
MUC13
C6orf52
RCAN2
TRIB2
GPR161
ID4
SORBS1
APCDD1
PRSS2
SLC46A1
PLK4
TFPI
SERPINE1
MX2
NEO1
KRAS-S181D signature FDR<0.01
KRAS-S181A signature FDR<0.05
Pearson's coefficient
1
n.s.
-1
b
D vs S FDR<0.01
UGT1A1
D signature
CRC T vs NT
A vs S FDR<0.05
A signature
up
down
n.s.
c
HNF4G
P-value: 0.006384
ID4
P-value: 0.02702
SERPINE1
P-value: 0.001185
NEO1
P-value: 0.01898
DFS probability
Time (months)
Quartile 1 (< 5.399)
Quartile 2 + 3 (>= 5.399 to < 6.414)
Quartile 4 (>= 6.414)
Quartile 1 (< 4.351)
Quartile 2 + 3 (>= 4.351 to < 5.266)
Quartile 4 (>= 5.266)
Quartile 1 (< 5.228)
Quartile 2 + 3 (>= 5.228 to < 6.495)
Quartile 4 (>= 6.495)
Quartile 1 (< 5.768)
Quartile 2 + 3 (>= 5.768 to < 6.313)
Quartile 4 (>= 6.313)